Environmental Science and Pollution Research (2023) 30:118736–118753
https://doi.org/10.1007/s11356-023-30536-2

RESEARCH ARTICLE

Electrochemically enhanced iron oxide–modified carbon cathode toward improved heterogeneous electro-Fenton reaction for the degradation of norfloxacin

Géssica de Oliveira Santiago Santos[1] · Lorena Athie Goulart[1] · Isaac Sánchez-Montes[1] · Ronaldo Santos da Silva[2] · Marcos Roberto de Vasconcelos Lanza[1]

Received: 5 July 2023 / Accepted: 13 October 2023 / Published online: 2 November 2023

Abstract

In this work, different iron-based cathode materials were prepared using two different approaches: a novel one-step approach, which involved the incorporation of iron oxide with Printex® L6 carbon/PTFE (PL6C/PTFE) on bare carbon felt (CF) and a two-step approach, where iron oxide is deposited onto CF previously modified with PL6C/PTFE. The results obtained from the physical characterization indicated that the presence of iron oxide homogeneously dispersed on the felt fibers with the CF 3-D network kept intact in the one-step approach; whereas the formation of iron oxide aggregates between the felt fibers for material obtained using the two-step approach. Among the iron oxide–based cathodes investigated, the iron-incorporated electrode exhibited the greatest efficiency in terms of the removal and mineralization of norfloxacin (NOR) under neutral pH (complete NOR removal in less than 30 min with around 50% mineralization after 90 min). The findings of this study show that the low cost and simple-to-prepare iron-modified carbon-based materials in HEF process led to the enhanced degradation of organic contaminants in aqueous solutions.

Keywords Heterogeneous electro-Fenton · Carbon felt · H_2O_2 electrosynthesis · Norfloxacin degradation · Mechanistic study

Abbreviations

AOPs	Advanced oxidation processes
CF	Carbon felt
ECSA	Electrochemically active surface ares
EF	Electro-Fenton
EAOPs	Electrochemical advanced oxidation processes
HEF	Heterogeneous electro-Fenton
GDE	Gas diffusion electrodes
MCF	Modified carbon felts
MCF-(3)	Modified carbon felt with ~3 mg cm^{-3} PTFE/PL6C
MCF-(6)	Modified carbon felt with ~6 mg cm^{-3} PTFE/PL6C
MCF/Fe-incorporated	Modified carbon felt with Fe incorporated in the structure
MCF/Fe-deposited	Modified carbon felt with with ~3 mg cm^{-3} PTFE/PL6C Fe deposited in the layer
NOR	Norfloxacin
PL6C/PTFE	Printex® L6 carbon/poly(tetrafluoroethylene)
TOC	Total organic carbon

Introduction

Over the past few years, water contamination by endocrine disruptors — mainly pharmaceutical compounds, has become a matter of great concern in our societies, and this has drawn considerable attention among researchers and other stakeholders worldwide (Kasonga et al. 2021; Pironti et al. 2021). The increasingly growing demand for pharmaceutical products (including antibiotics) intended for the treatment and prevention of diseases, ailments and

Responsible Editor: Guilherme Luiz Dotto

✉ Géssica de Oliveira Santiago Santos
gessicasantiago@usp.br

[1] São Carlos Institute of Chemistry, University of São Paulo, São Carlos, SP 13560-970, Brazil

[2] Department of Physics, Federal University of Sergipe, São Cristovão, SE 49100-000, Brazil

pains has given rise to a rampant use of these compounds and their haphazard disposal in water bodies; this has led to the frequent detection of these pharmaceutical substances in various aqueous matrices (Kovalakova et al. 2020). Norfloxacin (NOR) is a popular antibiotic which is widely used because of its high antimicrobial content; this compound has been detected in wastewater and other water bodies (Médice et al. 2021) and has been classified as a persistent contaminant due to its low biodegradability and toxicity to microorganisms. NOR has been found to pose serious risks to human health and to the ecosystem as it promotes the proliferation of resistant bacteria when present in aqueous systems (Michael et al. 2013). The presence of this kind of contaminants in water bodies has become a matter of great concern since conventional methods of water treatment have been found to be incapable of effectively removing these substances in water, thus leading to their accumulation in the environment (Li et al. 2021; Van Doorslaer et al. 2014).

Taking the above considerations into account, it is clear that there is an urgent need for the development of efficient treatment techniques which are capable of effectively degrading or removing antibiotics and other harmful contaminants from water/wastewater. In this context, electrochemical advanced oxidation processes (EAOPs) have emerged as highly efficient alternative methods for the treatment of contaminants due to their clean, environmentally friendly nature as well as their proven efficiency in treating water contaminated by recalcitrant compounds, mainly through the generation of hydroxyl radicals ($^{\bullet}$OH) (Ganiyu et al. 2021; Khan et al. 2020; Taoufik et al. 2021). Electro-Fenton (EF) process is regarded as one of the most economically attractive EAOPs (Brillas et al. 2009; Sirés and Brillas 2021). In this process, hydrogen peroxide (H_2O_2) is electrochemically generated and $^{\bullet}$OH species are formed via the electrochemically assisted Fenton reaction (involves the combination of H_2O_2 and ferrous ions) [$H_2O_2 + Fe^{2+} \rightarrow {}^{\bullet}OH + HO^- + Fe^{3+}$] (Brillas et al. 2009; Petrucci et al. 2016).

More recently, the use of heterogeneous electro-Fenton (HEF) process for the treatment of water has gained considerable traction among researchers as it allows the treatment to be performed at varying pH levels and provides one with the possibility of reutilizing the heterogeneous catalyst for the conduct of consecutive analyses (Alizadeh and Rezaee 2022; Ghanbari et al. 2021; Jonoush et al. 2021; Wang et al. 2021). The successful application of the HEF process requires the use of highly efficient electrocatalysts with suitable properties (Jonoush et al. 2020, 2022). Bearing that in mind, the use of new cathodic materials with outstanding properties such as iron supported on carbonaceous materials in HEF processes has sparked the interest of researchers due to the high surface area of these materials (Han et al. 2022; Li et al. 2022). Carbon felt (CF) is a suitable material known to be characterized by good electronic conductivity and a sizeable number of active sites (Le et al. 2017). The modification of CF with carbon black and poly(tetrafluoroethylene) (PTFE) leads to the production of a highly efficient electrocatalyst with an enhanced ability to generate a huge amount of H_2O_2 compared to an unmodified CF (Zhang et al. 2020).

In general, a good iron-based catalyst supported on carbonaceous materials should possess the following desirable properties: elevated electrocatalytic activity, stability at different pH levels, reusability, and environmental compatibility (Luo et al. 2021). The main challenges encountered when it comes to the development of an efficient electrocatalyst for application in HEF processes are as follows: (i) the stability of the catalyst when the pH becomes acidic (leaching of iron species); and (ii) the complexity involving the preparation of the catalyst (Ganiyu et al. 2018). Under the HEF mechanism, the activation of H_2O_2 to generate $^{\bullet}$OH species may occur homogeneously through the Fe^{3+}/Fe^{2+} redox pair (under acidic pH conditions), or through the process catalyzed superficially by the metallic species $\equiv Fe^{III}-OH$ to $\equiv Fe^{II}-OH$, or through both, depending on the operating pH level (Wan and Wang 2017). Thus, further studies need to be conducted with a view to developing novel, highly efficient iron-based cathodes which are endowed with a considerable number of sites for H_2O_2 electrolysis (oxygen reduction reaction via the $2e^-$ mechanism); this is because the efficiency of the HEF process is primarily dependent on the rapid activation of the electrogenerated H_2O_2 by the iron species supported on the electrode surface (Wang et al. 2021).

With that in mind, the present study reports the development and application of novel iron-based cathodes in HEF process using two different approaches: (i) iron oxide is incorporated into a carbon matrix on CF surface; and (ii) iron oxide is deposited directly on CF previously modified with a carbonaceous matrix. Based on the application of the two approaches, we expect to obtain an efficient and reusable cathode capable of operating under a near-neutral pH range. The performance of the cathodes will be investigated by monitoring H_2O_2 generation and activation under different synthesis conditions. To evaluate the efficiency of the HEF process, the degradation of NOR and its by-products will be monitored by high-performance liquid chromatography (HPLC), ion chromatography (IC), and total organic carbon (TOC). Finally, the mechanisms involving the oxidation of NOR based on the application of the proposed materials will be elucidated.

Experimental section

Materials

The following materials were employed in the experiments: Norfloxacin (99%), Iron (III) chloride hexahydrate

($FeCl_3 \cdot 6H_2O$) (97%), ethylene glycol (99.8%), citric acid (99.5%), *n*-Butanol (99.5%), ammonium molybdate, and short-chain carboxylic acid standards (a.r.; including oxalic and formic acids) — all the materials were purchased from Sigma Aldrich. Carbon felt (CF), Printex® L6 carbon (PL6C) powder, and poly(tetrafluoroethylene) (PTFE) (60% — aqueous dispersion), used in the experiments, were acquired from LMTerm, Evonik Ltd., and Dupont®, respectively. Other reagents used in the experiments were as follows: potassium sulphate (>99%; Vetec), nitric acid (65%; Synth), sulfuric acid (98% Neon), sodium bicarbonate (>99%; J.T. Baker), sodium carbonate (>99%; J.T. Baker) and acetonitrile (HPLC grade, J.T. Baker). All chemicals were used as received. Ultrapure water (Millipore® Milli-Q system, ρ≥ 18.1 MΩ cm) was used to prepare the solutions.

Preparation of the cathodes

CF with dimension of 4 cm × 5 cm × 1 cm (length × width × height) was used to prepare the modified carbon felts (MCF). PLC6/PTFE dispersion in the proportion of 25:75 was prepared by sonicating a mixture of 0.3 g of PL6C, 1.5 g of PTFE dispersion, 30 mL of ultrapure water and *n*-Butanol (3% *V*/*V*) in an ultrasonic bath. The dispersion was then loaded onto the CF which was immediately calcined in an oven at 360 °C for 1 h at a heating rate of 10 °C min^{-1} to prepare the MCF (Yu et al. 2015).

To optimize the mass loading of PL6C/PTFE, the MCF cathodes were prepared by the deposition of one and two layers of the dispersion. The deposition with one and two layers (cycles) of dispersion yielded 60 mg (~3 mg cm^{-3}) and 120 mg (~6 mg cm^3) electrodes, respectively; the electrodes were then subjected to calcination. To determine the final mass deposited, the initial mass of the CF substrate was subtracted from the mass obtained after calcination ($m_{deposited} = m_{initial} - m_{after\ calcination}$). The value obtained was then divided by the volumetric area of CF (20 cm^3). These electrodes will be denoted hereinafter as MCF-(3) and MCF-(6).

To obtain the iron-based MCF electrodes, two different approaches were employed: (1) the iron oxide was incorporated on the felt fibers by soaking the CF in a previously prepared dispersion containing PL6C, PTFE and $FeCl_3 \cdot 6H_2O$ (one-step approach); and (2) the iron oxide was deposited on CF previously modified with PL6C/PTFE through thermal decomposition of a polymeric iron precursor (prepared based on the procedure reported in (Santos et al. 2020)) (two-step approach). The cathodes will be denoted hereinafter as MCF/Fe-incorporated and MCF/Fe-deposited for the one-step and two-step approaches, respectively.

Physical characterization

The surface morphology of the cathodes was characterized by scanning electron microscopy using scanning electron microscope (SEM; JEOL model JSM 6510 V) equipped with an X-ray detector for EDS spectroscopy. X-ray diffraction (XRD; Rigaku diffractometer RINT 2000/PC) analysis was carried out using CuKα radiation (wavelength = 1.5406 Å) in a scanning interval of 2Θ range between 20 and 60°, in continuous scan mode, with steps of 0.02° min^{-1}. The crystalline phases were indexed using the X'Pert High Score Plus software (version 2.2.2) according to database of Joint Committee on Powder Diffraction Standards (JCPDS) database. To verify the hydrophobicity of the materials, contact angle values were recorded using a tensiometer (Teclis Tracker, IT Concept). A 3 µL volume of water was dropped on the surface of the materials and the contact angle between them was estimated.

Electrochemical characterization

The electrochemical characterization (linear sweep voltammetry (LSV), cyclic voltammetry (CV) and electrochemical impedance spectroscopy (EIS)) of the materials were performed using potentiostat/galvanostat (MetrohmAutolabPGSTAT-128N). The measurements were performed using a one-compartment three-electrode cell equipped with the prepared cathodes (used as working electrodes), a dimensional stable anode (DSA®) composed of RuO_2-TiO_2 (used as counter electrode), and Ag/AgCl (3 mol L^{-1} KCl) — used as reference electrode. In all the analyses, 0.05 mol L^{-1} K_2SO_4 solution at pH 7 (without adjustment) was used as supporting electrolyte. The oxygen reduction reaction (ORR) was evaluated by LSV using scan rate of 10 mV s^{-1} and potential interval of −1.3–0 V *vs* Ag/AgCl (3 mol L^{-1} KCl). EIS analysis was conducted based on the application of different voltages in the frequency range of 1000 to 0.01 Hz, with AC amplitude of 5 mV.

H_2O_2 electrogeneration and NOR degradation

The experiments involving H_2O_2 electrogeneration and the degradation of NOR were carried out in a one-compartment cell (batch operation mode) using potentiostat/galvanostat (MetrohmAutolab PGSTAT302). DSA® (4 cm^2) and Ag/AgCl (3 mol L^{-1} KCl) were used as counter (anode) and reference electrodes, respectively. Unmodified (CF) and modified (MCF-(3), MCF-(6), MCF/Fe-incorporated and MCF/Fe-deposited) carbon felts of 20 cm^2 (geometric area) prepared according to the procedure described above were used as cathodes. All the experiments were performed using 200 mL of 0.05mol L^{-1} K_2SO_4 solution (pH ~7) under continuous agitation with the aid of a magnetic stirrer (500

rpm), under applied temperature of 25 °C. A continuous flow of O_2 was fed into the electrolyte at a flow rate of 1 L min^{-1} during the experiments.

The experiments involving the electrogeneration of H_2O_2 were performed using the MCF-(3) and MCF-(6) cathodes, with the application of different electric currents of 0.1, 0.15 and 0.3 A (*i.e.*, j = 5, 7.5 and 15 mA cm^{-2}, respectively) relative to the geometric area of the cathode (the values of j in terms of volumetric area are equivalent). After the optimization of the applied current, 0.15 A (7.5 mA cm^{-2}) was chosen for the conduct of subsequent studies on H_2O_2 electrogeneration using the iron oxide–based cathodes. In this step, an analysis was conducted in order to evaluate the influence of pH on the amount of electrogenerated oxidant using MCF-(3), MCF/Fe-deposited and MCF/Fe-incorporated. Finally, the degradation of NOR (63 µmol L^{-1}) was evaluated under the optimal conditions obtained.

NOR removal and mineralization analyses

The concentration of electrogenerated H_2O_2 was measured after adding 0.5 mL of the sample to 4.0 mL of 2.4×10^{-3}mol L^{-1} ammonium molybdate solution — which turns into a yellowish complex in the presence of H_2O_2 (with absorbance at 350 nm) (Forti et al. 2007). The electrogenerated H_2O_2 was then quantified spectrophotometrically using UV–vis spectrophotometer (Shimadzu UV-1900).

The degradation of NOR was monitored by HPLC/UV-DAD detector using HPLC equipment, Shimadzu model LC-20AT, coupled to an SPD-20A detector. A Phenomenex reverse-phase C18 column (250 mm × 4.6 mm, 5 µm particle size) was used as the stationary phase and a mixture of 50:50 acetonitrile/acidified water (5% formic acid) was used as mobile phase in an isocratic mode. The conditions applied for this analysis were as follows: flow rate of 0.8 mL min^{-1}, injection volume of 20 µL, detection wavelength of 275 nm, and oven temperature of 40 °C. The degree of mineralization was evaluated using Shimadzu TOC analyzer (model TOC-VCPN). The carboxylic acids were identified by ion chromatography using Metrosep Organic Acids 250/7.8 column, with the application of 0.5 mmol L^{-1} H_2SO_4 (flow rate of 0.5 mL min^{-11}) as eluent, injection volume of 20 µL, and column temperature of 60 °C. The retention time of formic acid and acetic acid was compared to that of the standards which have been previously analyzed. Isopropanol was employed as quenching agent to investigate the role of hydroxyl radicals in the degradation mechanism of norfloxacin where the second-order rate constants with the hydroxyl radical is $k = 2.8\times10^9$ M^{-1} s^{-1}. (Liang and Su 2009). The iron leached was quantified using the orthophenantroline complexometric method (Murti et al. 1970).

The percentage of current efficiency (CE) was calculated based on Eq. (1), where 2 corresponds to the number of electrons required for oxygen reduction, F is the Faraday constant (96,487 mol^{-1}), $C_{H_2O_2}$ is the H_2O_2 concentration in mol L^{-1}, V_s is the volume of solution in L, I is the applied current in A, and t is the time of electrolysis (s) (Fortunato et al. 2020b).

$$\mathrm{CE}_{H_2O_2}\,(\%) = \frac{2\,FC_{H_2O_2}V_S}{It}\times 100\% \tag{1}$$

The energy consumption (EC_{H2O2}) was derived from Eq. (2), where E_{cell} is the average of cell potential (V), I is the applied current (A), t is the time of electrolysis (hour), $C_{H_2O_2}$ is the concentration of H_2O_2 (mg L^{-1}), and V_s is the volume of solution (L) (Barros et al. 2015b).

$$\mathrm{EC}\left(\mathrm{kWh\ kg^{-1}}\right) = \frac{1000\,E_{cell}It}{C_{H_2O_2}V_S} \tag{2}$$

The energy consumption (EC_{TOC}) per TOC removal was calculated based on Eq. (3), where E_{cell} is the cell potential (V), I is the applied current (A), t is the electrolysis time (s), V_s is the volume of solution (L), and Δ[TOC] is the change in TOC concentration (mg L^{-1}) (Fortunato et al. 2020a).

$$\mathrm{EC}_{\mathrm{TOC}}\left(\mathrm{kWh\ g^{-1}}\right) = \frac{E_{cell}It}{V_S\Delta[TOC]} \tag{3}$$

The figure-of-merit, specific electrical energy (E_{EO}), corresponds to the electrical energy (kW h^{-1}) required to decrease the concentration of the contaminant in one order of magnitude. The E_{EO} was used to compare the data obtained from the application of other AOPs in terms of cost-efficiency based on Eq. (4), where E_{cell} (V) is the average cell potential, I is the current applied (A), V_s is the volume of solution (L), and k_1 is the pseudo-first-order constant (min^{-1}) (Bolton et al. 1996; Lanzarini-Lopes et al. 2017).

$$\mathrm{E_{EO}}\left(\mathrm{kWh\ m^{-3}order^{-1}}\right) = \frac{38.4\times10^{-4}E_{cell}I}{V_Sk_1} \tag{4}$$

Results and discussion

Optimization of the amount of PL6C used in H_2O_2 electrogeneration

Physical and electrochemical characterization

SEM analyses of the unmodified CF and modified MCF-(3) and MCF-(6) cathodes were performed in order to investigate the effect of PL6C/PTFE loading on the morphology of the materials. Figure 1a–c shows that the PL6C/PTFE mixture is homogenously deposited on the carbon fibers with some

agglomerated regions. The EDS analysis of the regions of each material showed the presence of carbon on pure CF; as expected, after modification with PL6C/PTFE, the modified materials exhibited the presence of fluorine element from PTFE (which has $(C_2F_4)_n$ composition) (Karatas et al. 2022; Rofaiel et al. 2012).

CV and LSV techniques were applied for the electrochemical characterization of the materials (Fig. 1d–e); these analyses were performed in order to evaluate the effect of the catalyst loading on the electrochemical properties of the cathodes. The electrochemically active surface area (ECSA) of MCF-(3) and MCF-(6) was determined as the relative measure of the voltammetric charge by integrating the CV curves in the range of −1.4–0 V *vs* Ag/AgCl at 20 mV s^{-1} (Fig. 1d). As can be observed in Fig. 1, the ECSA values obtained were quite close to each other; this means that an increase in PL6C/PTFE loading does not lead to a significant increase in the active sites for electrochemical reaction

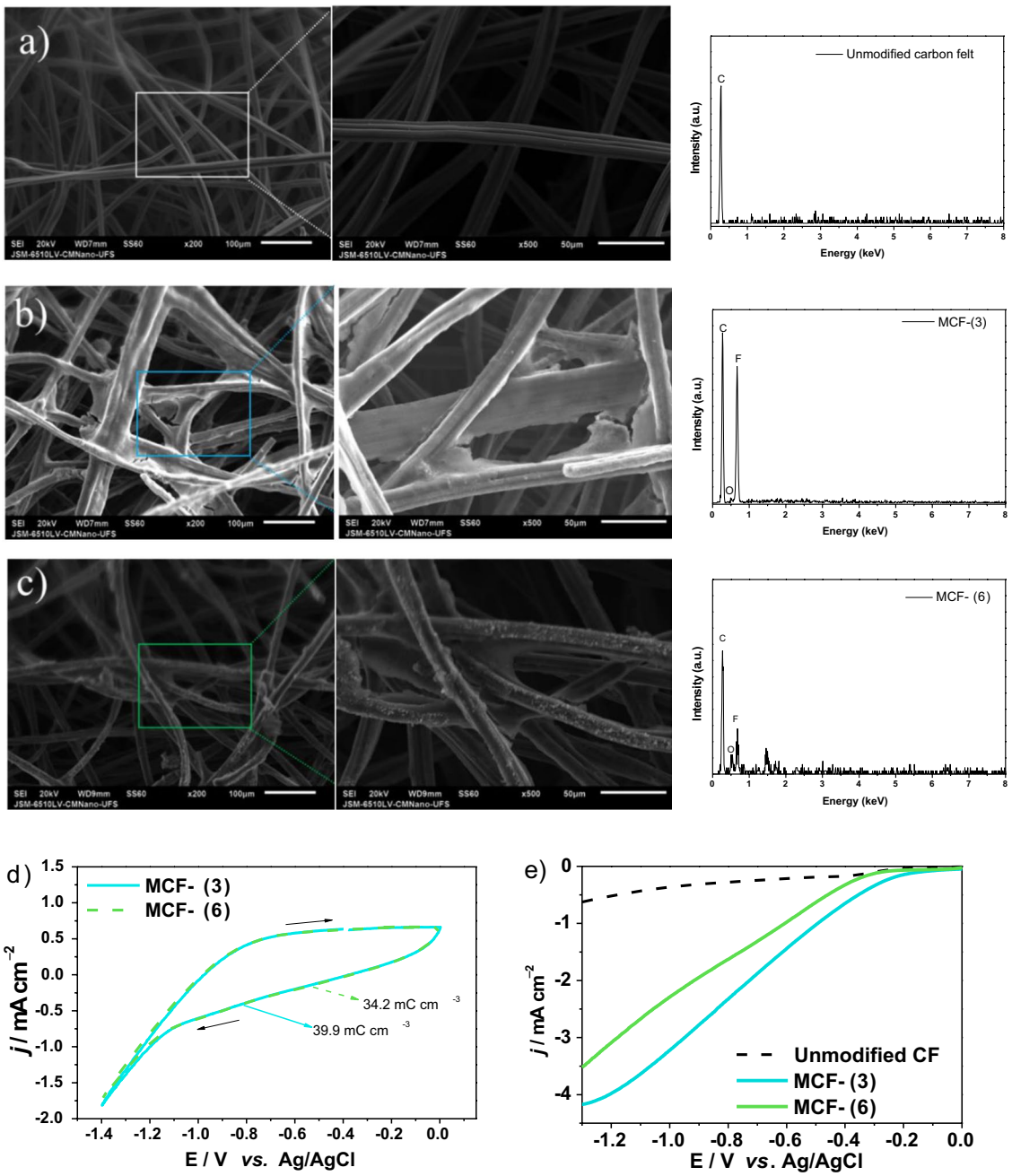

Fig. 1 SEM images and EDS spectra of: (**a**) pure CF, (**b**) MCF-(3), (**c**) MCF-(6) and (**d**) cyclic voltammetries and (**e**) linear sweep voltametries of CF, MCF-(3), MCF-(6) recorded at 20 mV s^{-1} in 0.05 mol L^{-1} K_2SO_4

To gain a better understanding of the ORR on the CF, MCF-(3) and MCF-(6) cathodes in the system studied at neutral pH, LSV measurements were performed in the negative region (Fig. 1e). The results obtained from the LSV measurements showed that both MCF cathodes presented relatively higher currents for ORR compared to the unmodified CF. This outcome is in line with the results obtained in previous studies reported in the literature which showed that the modification of graphite felt with carbon black/PTFE led to improvements in the electrocatalytic activity for O_2 reduction and conductivity of the material (Huang et al. 2021; Yu et al. 2015). The electrode containing higher PL6C/PTFE loading (*i.e.*, MCF-(6)) exhibited relatively lower current density compared to the MCF-(3); this points to a reduction in the active sites for O_2 reduction, which is likely to have led to the electrogeneration of lower amounts of H_2O_2.

Effect of applied current on H_2O_2 electrogeneration

The high number of sites for the electrogeneration of H_2O_2 under the $2e^-$ ORR mechanism is found to be of great importance in the HEF process; this is because the efficiency of the process in terms of the degradation of organic pollutants is deeply related to the rapid activation of H_2O_2 by the heterogeneous catalyst (Zhou et al. 2019). Fig. 2 shows the concentration of H_2O_2 electrogenerated in 60 min of electrolysis based on the application of the MCF-(3) and MCF-(6) electrodes at different current densities using 0.05 mol L^{-1} K_2SO_4 solution as electrolyte solution. Primarily, the formation of H_2O_2 occurs via the electrochemical reduction of oxygen dissolved in the solution based on chemical Equation (5) (Perry et al. 2019). Looking at Fig. 2a, it is clear that H_2O_2 accumulation follows a pseudo-zero order kinetics, which is reflected by the linear increase in concentration observed in the first 30 min of electrolysis (the same profile can be observed in Fig. 2b). After 30 min of electrolysis, H_2O_2 electrogeneration can be found to have stabilized; this pattern of behavior has been widely documented in the literature, and it is attributed to different side/parallel reactions that may affect the H_2O_2 electrogeneration process. These parallel reactions include the following: self-decomposition (Eqs. (6)–(8)), cathodic reduction to water (Eq. (9)) or oxidation to oxygen at the anode, to name a few (see Eq. (10)) (Brillas et al. 1995; Carneiro et al. 2015; Samanta 2008).

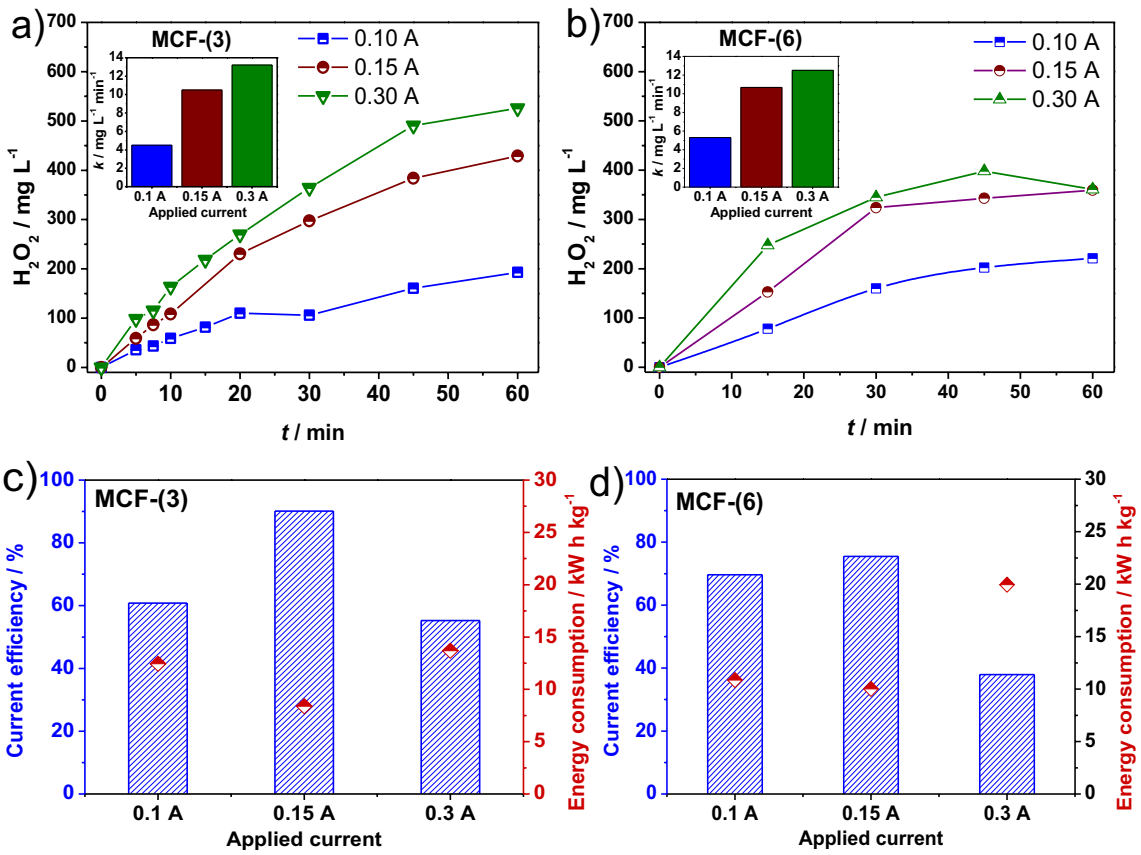

Fig. 2 Effect of PL6C/PTFE loading on H_2O_2 electrogeneration (**a**, **b**) and current efficiency and energy consumption (**c**, **d**) at different current densities. Electrolyte solution: 0.05 mol L^{-1} K_2SO_4 at pH 7

$$O_{2(g)} + 2H^+ + 2e^- \rightarrow H_2O_2 \quad (5)$$

$$2H_2O_2 \rightarrow 2H_2O + O_2 \quad (6)$$

$$H_2O_2 \leftrightarrow HO_{2-} + H^+ \quad (7)$$

$$H_2O_2 + HO_{2-} \rightarrow H_2O + O_2 + OH^- \quad (8)$$

$$H_2O_2 + 2H^+ + 2e^- \rightarrow 2H_2O \quad (9)$$

$$H_2O_2 - 2e^- \rightarrow O_2 + 2H^+ \quad (10)$$

The kinetics of H_2O_2 electrogeneration was analyzed for the MCF-(3) and MCF-(6) electrodes taking into account the first 30 min of electrolysis. The results obtained showed that MCF-(3) recorded the following kinetics values: 4.5, 10.5 and 13.2 mg L^{-1} min^{-1}, at the applied current densities of 0.1, 0.15 and 0.3 A, respectively. Interestingly, by doubling the PL6C/PTFE loading MCF-(6), the kinetics values obtained were 5.3, 10.7 and 12.5 mg L^{-1} at the applied current densities of 0.1, 0.15 and 0.3 A, respectively; this shows that both cathodes recorded similar amounts of electrogenerated H_2O_2.

The current efficiency (CE) and energy consumption (EC) of the MCF-(3) and MCF-(6) electrodes were also calculated (see Fig. 2c–d). As can be observed, the highest current efficiencies were obtained by the application of current density of 0.15 A, with MCF-(3) and MCF-(6) recording 90.1% and 75.5% of current efficiency, respectively. With regard to energy consumption, the lowest amounts of energy consumed by MCF-(3) and MCF-(6) were 8.4 and 10.0 kWh kg^{-1}, respectively. These results point to the following: (i) the applied current of 0.15 A is the most suitable current for H_2O_2 electrogeneration; and (ii) the MCF-(3) electrode exhibited better performance in terms of CE and EC. In view of that, the MCF-(3) electrode was chosen as the optimal mass loading as it is able to provide sufficient electrochemical active area and diffuse the amount of O_2 required for H_2O_2 electrogeneration. These data are in agreement with those discussed above related to the physical and electrochemical characterization of the materials (Fig. 1).

Effect of iron supported on PL6C/PTFE in H_2O_2 electrogeneration

Physical and electrochemical characterization

Over the past few years, there has been a considerable interest among researchers in the development of highly effective, low-cost iron oxide-based cathodes for use in HEF systems under neutral operating environment (Ganiyu et al. 2018; Perry et al. 2019). In the present study, after the analysis of the optimal PL6C/PTFE loading, the iron oxide-based cathodes were prepared by modifying the MCF-(3) cathode. The images obtained from the SEM analysis pointed to the successful deposition (MCF/Fe-deposited) and incorporation (MCF/Fe-incorporated) of iron oxide onto the CF fibers — see Fig. 3a–b. In a recent study conducted by Huang et al. (2021), with the aid of SEM images, the authors showed that the modification of graphite felt with a mixture of iron-manganese binary oxide, activated carbon, carbon black and PTFE led to a good distribution of the particles formed over the fibers of the graphite felt electrode (Huang et al. 2021). Under the two approaches employed in our present study, the presence of iron and oxygen was detected through EDS mapping images; this is clearly indicative of the successful deposition or incorporation of the iron on the PL6C/PTFE material. The XRD patterns obtained for the unmodified CF and the three MCF cathodes (Fig. 3e) exhibited diffraction peaks related to carbon (Huang et al. 2021; Su et al. 2019), and the two iron oxide–based cathodes prepared were composed of Fe_2O_3 (JCPDS Card No 96-9770) (Su et al. 2019); however, only the Fe-incorporated cathode presented a peak related to zero valent iron (Fe^0) (JCPDS Card No 06-0696). The aforementioned results are in agreement with the findings reported in previous studies related to the development and application of iron-based cathodes (Huang et al. 2021).

The analysis of contact angle (CA) was carried out in order to investigate the wettability of the cathodes (Fig. SM1). In this technique, liquid drop (usually water) is placed on a solid surface, forming an angle based on the gas-liquid-solid interface — this is referred to as the contact angle (Θ). Materials with CA values (Θ) > 90° have low degree of wettability (*i.e.*, hydrophobic surface), and the materials with Θ values > 150° are found to be superhydrophobic in nature, while those with Θ values < 90° are typically hydrophilic in nature (Kim et al. 2014). The results obtained from the analysis of the contact angle of the materials reflected the following tendency: ΘCF < ΘMCF/Fe-incorporated < ΘMCF-(3) < ΘMCF/Fe-deposited. These results show that the wettability of the materials changes according to the modification of MCF; in other words, the CA of the CF is found to increase after modification — as expected by the presence of PTFE. The MCF/Fe-incorporated exhibited the lowest degree of wettability among the modified cathodes; this may be attributed to the formation of Fe_2O_3 nanoparticles on the felt fibers. In contrast, the MCF/Fe-deposited exhibited the highest CA values; this may be attributed to the formation of Fe_2O_3 as deposits between the felt fibers.

Mohamed et al. developed an efficient modified anode via the deposition of Fe/Fe_2O_3 nanoparticles for energy production and wastewater treatment; the authors found that

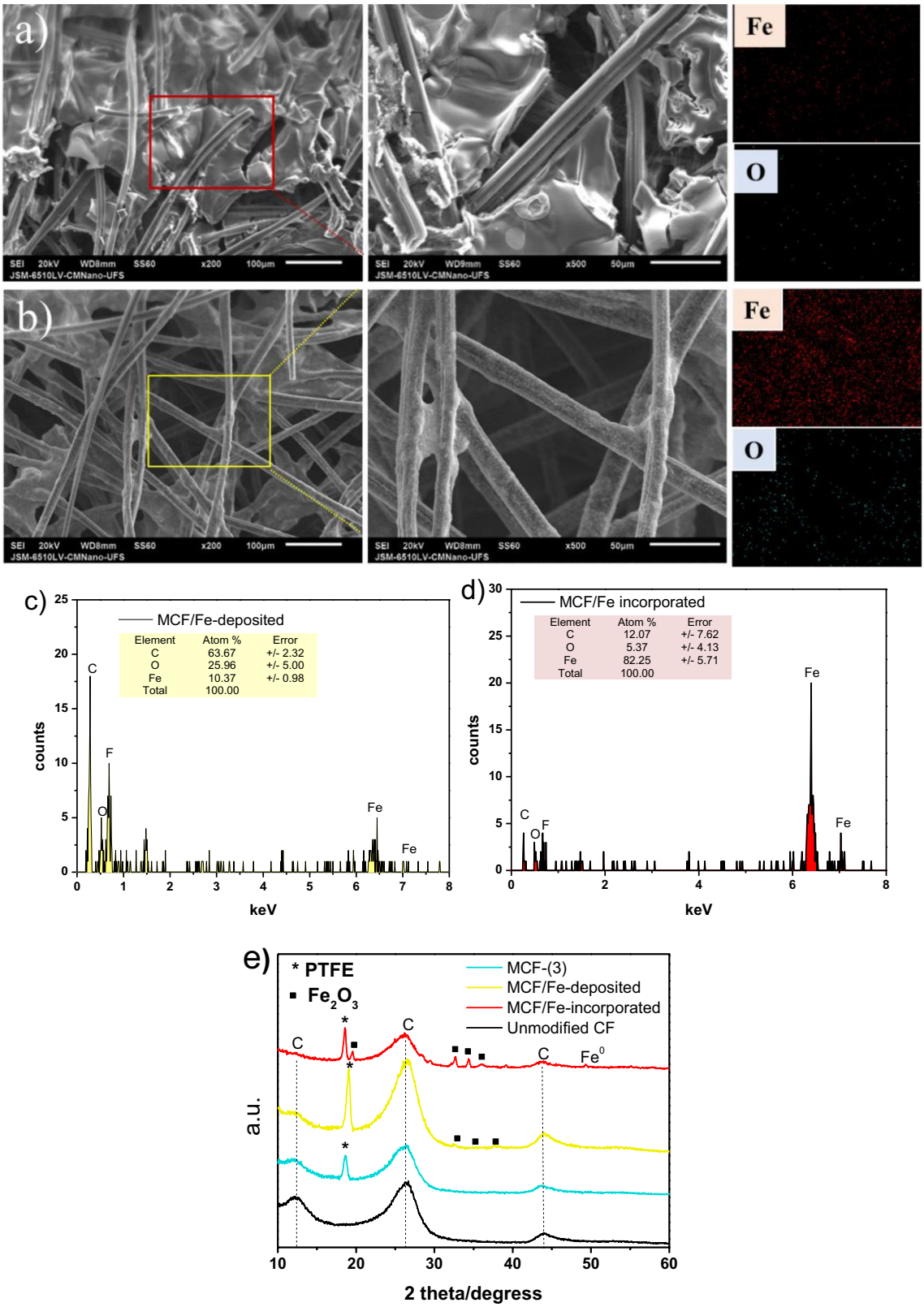

Fig. 3 SEM images and EDS mapping images of: (**a**) MCF/Fe-deposited and (**b**) MCF/Fe-incorporated (**b**); EDS spectra (elemental analysis) of (**c**) MCF/Fe-deposited and of (**d**) MCF/Fe-incorporated; and XRD patterns obtained for the unmodified CF substrate and CF modified with and without iron oxide (prepared by deposition or incorporation)

the wettability of carbonaceous materials, including carbon felt, was enhanced after modification with iron/iron oxide (Mohamed et al. 2018).

The electrochemical behavior of the cathodes was evaluated using CV and EIS. CV profiles obtained for MCF, MCF/Fe-deposited and MCF/Fe-incorporated are shown in Fig 4a. Looking at the CV profile of the iron oxide–modified cathodes, one can observe the presence of the Fe(II)/Fe(III) redox couple with the anodic peaks at around 0.6–0.8 V *vs* Ag/AgCl and the cathodic peaks at 0.1–0.2 V *vs* Ag/AgCl (Kabtamu et al. 2018). Among the iron oxide-modified cathodes, the MCF/Fe-incorporated exhibited the largest voltammetric area with extremely high currents for oxidation and reduction reactions. As pointed out in the literature, the electrochemically active surface area (ECSA) is a useful tool for measuring the intrinsic electrochemical activity of the materials investigated (Ren et al. 2020). The ECSA of MCF, MCF-(3) and MCF-(6) was calculated by the double layer capacitance method (Fig. 4b–c) — this is a common technique used to study the electrochemical activity of carbon-based materials (Cordeiro-Junior et al. 2020; McCrory et al. 2013). The results obtained from this analysis showed that the MCF/Fe-incorporated electrode exhibited the greatest surface area, followed by the MCF/Fe-deposited electrode; the iron oxide-free MCF exhibited the lowest surface area. These results show that the modification of the MCF with iron oxide leads to a significant improvement in the surface area of the material.

EIS measurements were performed using different MCF electrodes applied in 0.05 mol L^{-1} K_2SO_4 (electrolyte solution) at different potentials (Fig. SM2a–c). The values related to the ohmic resistance of the electrolyte solution, electrodes and contacts (R_Ω) as well as the charge transfer resistance (R_{ct}) were obtained from the Nyquist diagrams; these values help evaluate the conductivity of the materials investigated. These parameters related to the adjustment of the EIS data are shown in Table 1.

The polarization voltages applied for the EIS measurements were chosen based on negative LSV curves and the corresponding Nyquist plots obtained can be

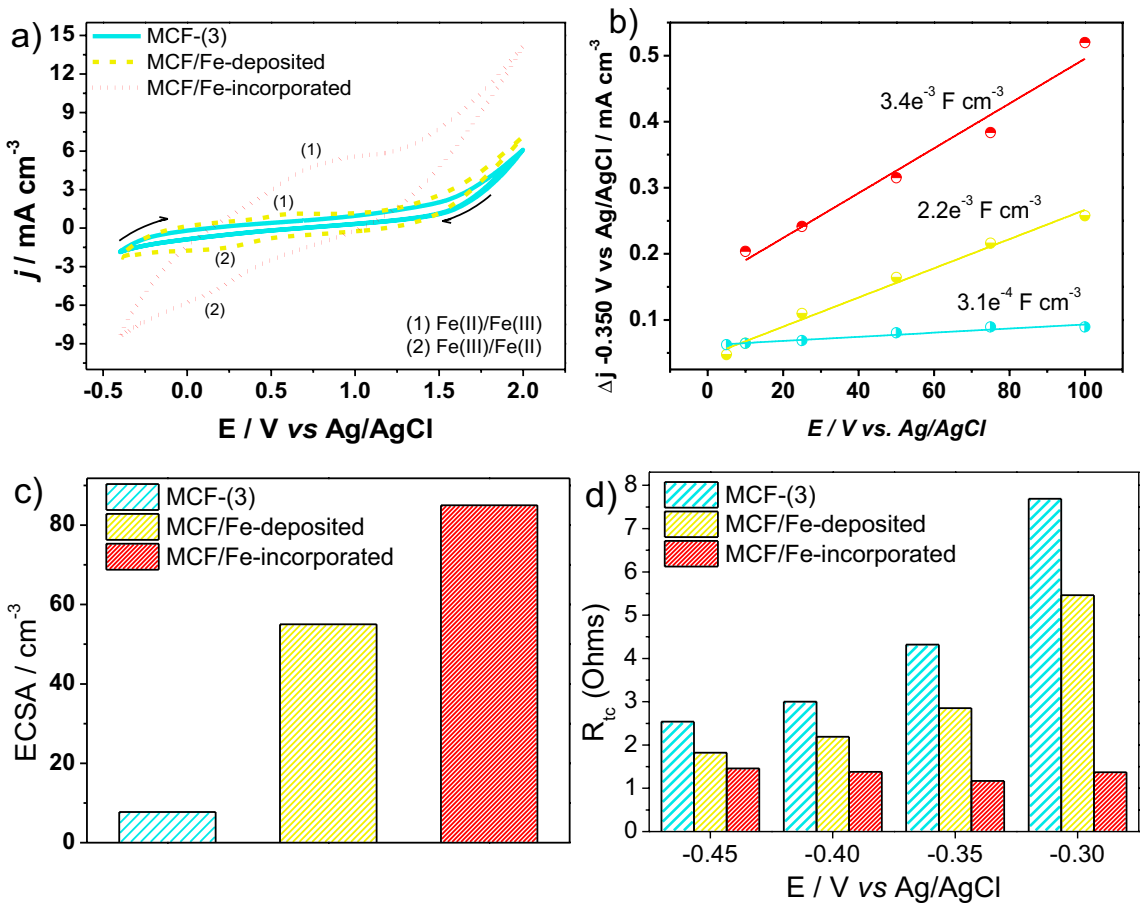

Fig. 4 CV curves obtained for the modified CF at scan rate of 50 mV s^{-1} (**a**), with capacitive current density average at −0.35 V *vs* scan rate (**b**); ECSA for the different cathodes (**c**) and charge transfer resistance obtained from the application of different polarization voltages (**d**). Conditions: 0.05 mol L^{-1} K_2SO_4 at pH 7 employed as electrolyte

found in Fig. SM2a–c. The voltages applied varied from the ORR onset potential (−0.3 V) to more negative values (−0.35, −0.40, and −0.45 V). Both the MCF/Fe-deposited and MCF/Fe-incorporated (in particular) exhibited lower R_{ct} values (Fig. 4d); this behavior may be attributed to the ion redox reaction of iron species that occur on the electrode surface. It has been well documented in the literature that the main functional groups typically found in carbonaceous matrix — commonly observed by X-ray photoelectron spectroscopy or Fourier transform infrared spectroscopy techniques, are ether (–C–O), carboxyl –COOH, (–C–OH), carbonyl (–C=O) and hydroxyl (–OH) groups (Abaalkhail et al. 2022; Cordeiro-Junior et al. 2020; Paz et al. 2018; Wang et al. 2014; Ye et al. 2016). Thus, we assume that the iron ions gradually connect with the active sites on the fiber surface (*i.e.*,–OH, –COOH) to form C–O–Fe bonds; these bonds contribute to the electron transfer reactions, leading to lower R_{ct} values. The iron oxide-deposited cathode also exhibited a similar pattern of behavior; in other words, the possible formation of C–O–Fe bonds in the cathode led to relatively smaller R_{ct} compared to the unmodified MCF cathode although the R_{tc} values of the iron oxide deposited cathode were higher than that of the iron-incorporated cathode.

Effect of modifying CF cathode with iron on H_2O_2 electrogeneration at different pH values

An analysis was conducted in order to evaluate the effect of pH (3, 7 and 11) on the concentration of H_2O_2 electrogenerated in 90 min of electrolysis (Fig. 5). Interestingly, the application of neutral pH contributed toward the electrogeneration of higher amounts of H_2O_2, which is favorable in terms of efficiency when it comes to the removal of contaminants and the application of the HEF process under suitable pH conditions that are compatible with environmental systems. On the other hand, an increase in the pH value to 11 led to the production of the lowest amount of H_2O_2. Under basic condition, H_2O_2 coexists with hydroperoxide ion (HO_2^-); this compound has been reported to be involved in the auto-decomposition of H_2O_2 in strongly basic solutions (pH > 9) ($HO_2^- + H_2O_2 \rightarrow H_2O + O_2 + OH^-$) (Barros et al. 2015a). A previous study conducted by Zhou et al. based on the application of hydrazine-modified CF also showed that an increase in pH from 3 to 8.1 led to a decrease in the amount of electrogenerated H_2O_2 from 193.9 to 162.2 mg L^{-1}, respectively (Zhou et al. 2008); this finding is consistent with the results obtained in the present work — where the application of pH 11 led to a shift in the equilibrium of the reaction to H_2O_2 decomposition. It should be noted however that, other studies published in the literature have reported the production of higher amounts of H_2O_2 in basic medium, especially when gas diffusion electrodes are applied (GDE). Similarly, Soltani et al. showed that an increase in the pH value from 6 to 9 resulted in an increase in the amount of H_2O_2 electrogenerated from 66.52 to 122.6 μM (Soltani et al. 2013). Barros et al. also investigated H_2O_2 electrogeneration in alkaline medium based on the application of GDE with PL6C where they reported to have obtained good results in terms of H_2O_2 production with the consumption of relatively low amount of energy (Barros et al. 2015a). It is worth pointing out that in our present work, CF is employed as an immersed cathode; this is totally different from gas diffusion cathodes where O_2 is continuously injected through the cathode. The results obtained in this study show that the electrode performance at different pH values varies according to the nature of the cathode material and the modifications carried out in this material.

Based on the results obtained, it can be concluded that the modified carbon felts recorded their best performance at pH close to neutral, followed by acidic pH environment. These findings are in agreement with those reported by Yu et al. who showed that modifying the cathode with carbon

Table 1 EIS data obtained for the modified carbon felt cathodes at the following potentials: −0.3, −0.35, −0.4, and −0.45 V *vs* Ag/AgCl

Cathode	E / V *vs* Ag/AgCl	R_Ω/Ω	R_{ct}/Ω	Q_{dl}/F (10^{-2})	n_{dl}	χ^2 (10^{-4})
MCF-(3)	−0.30	2.54	7.69	1.46	0.69	1.8
	−0.35	2.51	4.32	1.58	0.70	0.28
	−0.40	2.51	3.00	1.34	0.72	0.67
	−0.45	2.51	2.54	1.21	0.74	0.82
MCF/Fe-deposited	−0.30	3.12	5.46	12.86	0.70	1.8
	−0.35	3.17	2.85	11.45	0.73	2.5
	−0.40	3.11	2.19	11.79	0.73	3.3
	−0.45	3.13	1.82	11.78	0.74	3.1
MCF/Fe-incorporated	−0.30	3.3	1.37	62.51	0.87	5.0
	−0.35	3.2	1.17	66.73	0.80	2.1
	−0.40	3.2	1.38	81.91	0.70	0.76
	−0.45	3.2	1.46	80.43	0.65	1.1

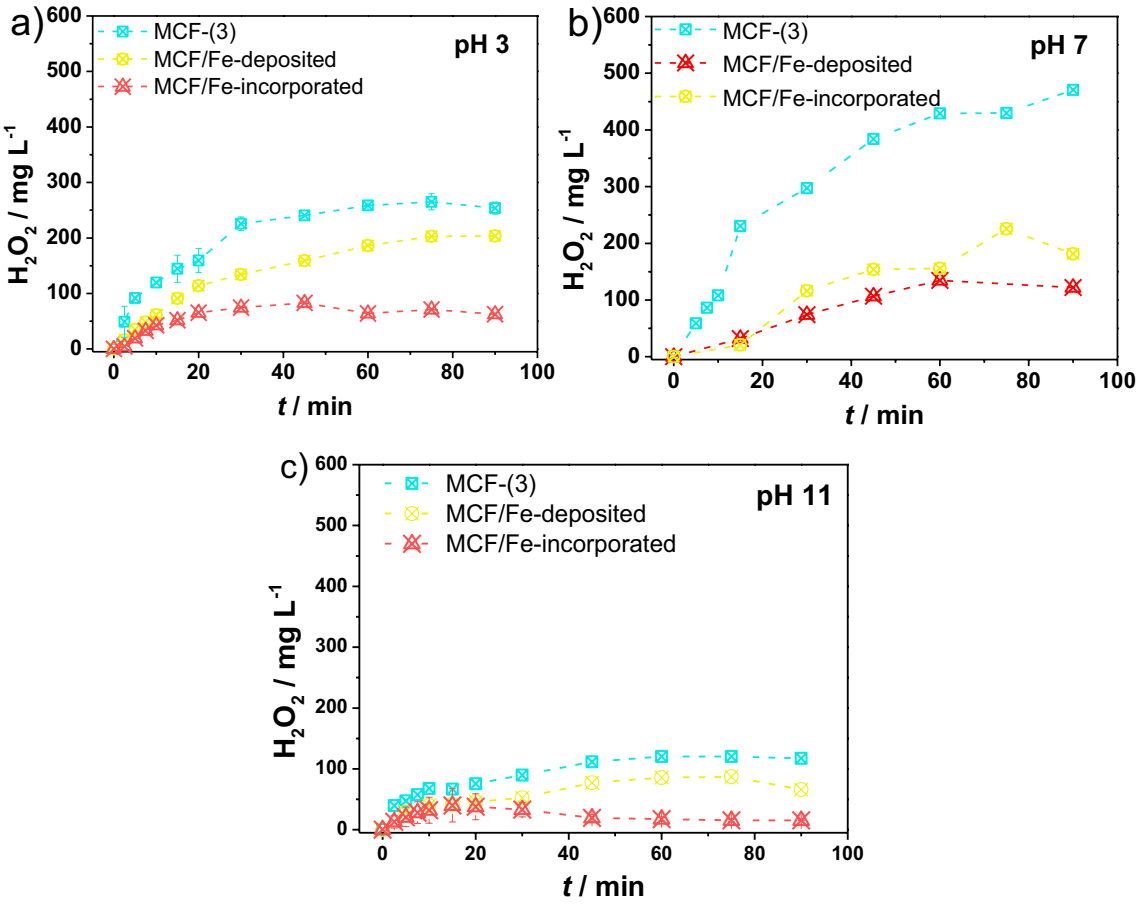

Fig. 5 Effect of the pH value on H_2O_2 electrogeneration based on the application of three different MCF cathodes. Conditions applied: 0.05 mol L^{-1} K_2SO_4 employed as electrolyte solution; pH values evaluated: 3, 7, and 11.

black contributed to a slight increase in H_2O_2 production at pH 7 (Yu et al. 2015).

NOR degradation

The performance of the MCF cathodes was investigated through degradation experiments using 63 µmol L^{-1} NOR in 0.05 mol L^{-1} K_2SO_4 at pH 7. As can be seen in Fig. 6a, the NOR removal percentages recorded for MCF and MCF-deposited in 90 min of treatment were 50.8% and 81.1%, respectively, while the MCF/Fe-incorporated cathode exhibited 100% of NOR removal in 30 min of experiment. These results help to confirm that the presence of iron oxide in the cathode enhances the efficiency of the HEF system applied under the H_2O_2 electrogeneration mechanism. In addition, the NOR removal process follows a pseudo-first-order kinetics model (inset in Fig. 6b). The degradation rate constant obtained for the MCF/Fe-incorporated cathode (k = 0.057 min^{-1}) was 5.34 and 3.54–fold higher than the value recorded for the iron oxide-free cathode (MCF) and the MCF/Fe-deposited cathode, respectively. A comparison of the iron oxide–deposited cathode with the iron oxide–incorporated cathode shows that the latter exhibited a 1.5-fold increase in NOR degradation rate constant relative to the former.

The application of the MCF/Fe-incorporated cathode resulted in TOC removal efficiency of 52.3% after 90 min of treatment under the HEF system; the application of the other two cathodes did not yield any change in TOC concentration (Table 2). Regarded as an important figure-of-merit, the electrical energy per order (E_{EO}) was used to compare the efficiency of different advanced electrochemical oxidation techniques (Bolton et al. 2001). As can be seen in Table 2, the application of the MCF/Fe-incorporated cathode under the HEF treatment process resulted in the lowest E_{EO} and the highest TOC removal efficiency. Two short-chain carboxylic acids were detected during the degradation process using the MCF/Fe-incorporated cathode (Fig. 6c); these acids, which consisted of formic and acetic acids, were found to be the terminal oxidation intermediates. The presence of formic and acetic acids has been previously reported in the literature during the degradation of other fluoroquinolone

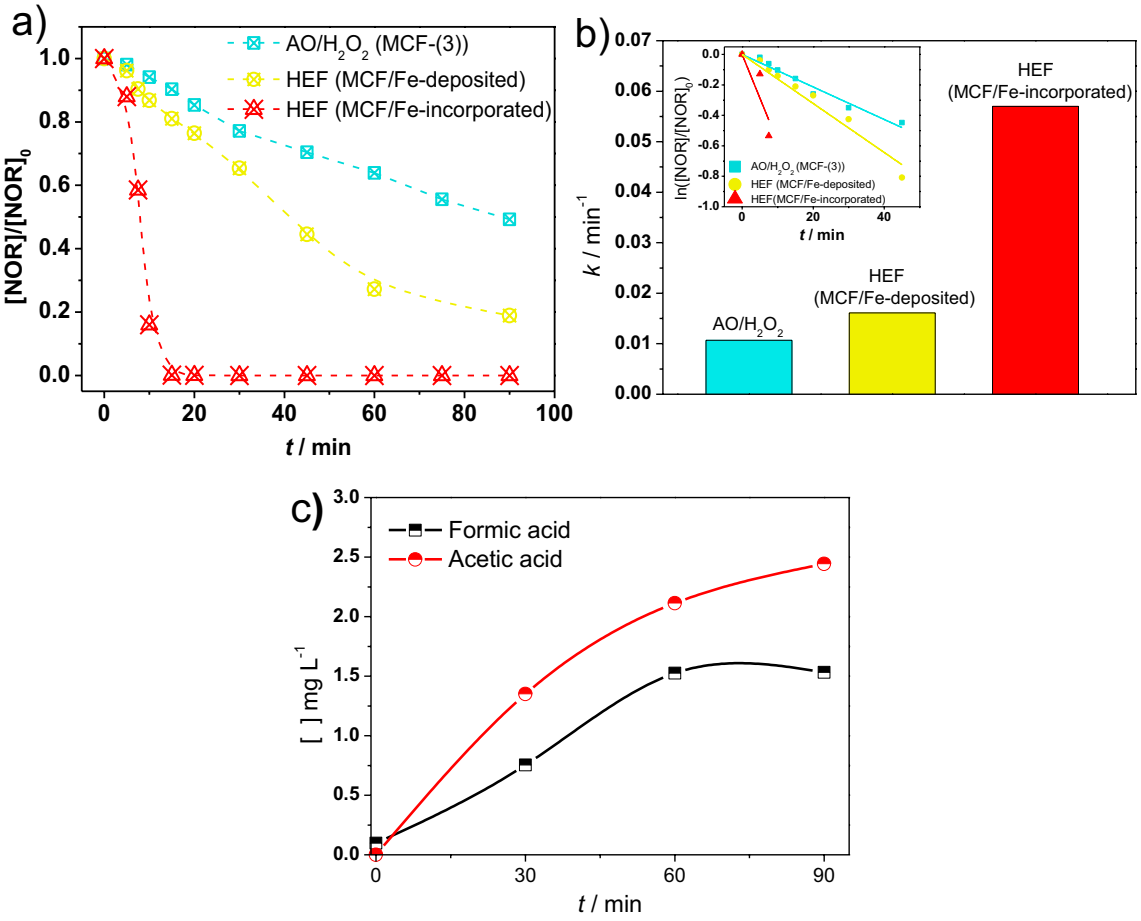

Fig. 6 Results obtained for (**a**) NOR decay, (**b**) degradation rate constants, and (**c**) short-chain carboxylic acids evolution during NOR removal under the HEF treatment mechanism based on the application of the MCF/Fe-incorporated cathode. Conditions applied — electrolyte solution: 0.05 mol L^{-1} K_2SO_4 at pH 7

Table 2 Percentages of total organic carbon (TOC) removed after 90 min of electrolysis and values related to electrical energy per order (EEO) obtained under the application of different treatment processes

Process	TOC removal (%)	E_{EO} (kW h m^{-3} $order^{-1}$)
AO-H_2O_2	0	21.98
HEF (with MCF/Fe-deposited)	0	12.27
HEF (with MCF/Fe-incorporated)	52.31	2.76

antibiotics, including levofloxacin, enoxacin, norfloxacin, and ciprofloxacin, under the application of the electro-Fenton process (Annabi et al. 2016; Barhoumi et al. 2015; Carneiro et al. 2020).

These results show that the application of the MCF/Fe-incorporated cathode at neutral pH generates the optimal conditions for the effective degradation/mineralization of NOR with high electrical energy consumption efficiency. As can be seen in Table 3 the degradation efficiency obtained from the application of the MCF/Fe-incorporated cathode under the HEF treatment process reported in the present work was found to be better than that obtained by previous studies reported in the literature which involved the use of other advanced oxidation processes (AOPs).

Mechanistic study

In HEF systems, the kinetics of the process is usually complex, depending on the nature of the catalyst (solubility) and the working pH; the most critical step in the process is the catalytic surface production of •OH species (Munoz et al. 2015). The mechanism that is widely accepted in the literature for the oxidation process under the HEF technique is similar to that of the classic homogeneous Fenton; the surface mechanisms involving this process can be found in Equations (11)–(16) below (Ganiyu et al. 2018; Wang et al. 2013). The mechanism of activation is initiated by the H_2O_2 electrogenerated (Eq. (1)) and by the reduction of $\equiv Fe^{III}$—OH (Eq. (11)) which occur simultaneously on the cathode. The surface complex

Table 3 Comparative analysis of NOR removal based on the application of different AOPs reported in the literature

AOP	Experimental conditions	Removal efficiency	Refs.
Electrochemical oxidation	**[Na_2SO_4]:** 2 g L^{-1} ***V*:** 250 mL **NOR_0:** 100 mg L^{-1} **Anode:** BDD; **Cathode:** Stainless steel ***j***: 83 mA cm^{-2}	100% NOR (60 min) k_{obs}: –	(Mora-Gómez et al. 2019)
Fenton	**[$MnFe_2O_4$]:** 0.6 g L^{-1} **[H_2O_2]** 200 mmol L^{-1} ***V*:** 100 mL **NOR_0:** 10 mg L^{-1}	90.6 % NOR (180 min) k_{obs}: –	(Wang et al. 2018)
Heterogeneous solar Photo-Fenton	**[Fe_3O_4-MWCNTs]:** 1.2 g L^{-1} **Light source:** Xenon light **pH:** 3 **[H_2O_2]** 0.098 mmol L^{-1}	89.9% (180 min) k_{obs}: –	(Shi et al. 2017)
Electro-Fenton	**[Na_2SO_4]:** 0.05 mol L^{-1} ***V*:** 250 mL **NOR_0:** 10 mg L^{-1} **Anode:** PbO_2/SnO_2; **Cathode:** Ag@ZOF-SS **Sacrificial anode:** iron flakes of 10 cm^2 **O_2 flow:** 0.2 L min^{-1} ***i***: 9mA	92.8% (150 min) k_{obs}: 0.017 min^{-1}	(Liu et al. 2022)
Hydrodynamic cavitation + H_2O_2	**Pressure:** 5.0 bar **NOR_0:** 10 mg L^{-1} **pH:** 3 **T:** 40 °C	96.4% (150 min) k_{obs}: –	(Yi et al. 2021)
Heterogeneous electro-Fenton	**[Na_2SO_4]:** 0.05 mol L^{-1} ***V*:** 200 mL **NOR_0:** 63 µmol L^{-1} **Anode:** DSA®-RuO_2-TiO_2 **Cathode:** MCF/Fe-incorporated **O_2 flow:** 1 L min^{-1} ***i***: 0.15 A (7.5 mA cm^{2-} cathode)	100% (20 min) k_{obs}: 0.057 min^{-1}	**This work**

BDD: boron-doped diamond; ***MWCNTs:*** Multiwalled Carbon Nanotubes loaded with stainless steel mesh; ***i:*** current intensity; ***j:*** current density

≡Fe^{III}—OH(H_2O_2) can be formed on the inner or external surface of the cathode (Eq. (12)). Also, the ≡Fe^{II}—OH($HO_2^{\bullet}$) can be formed via electron transfer (Eq. (13)) and be deactivated to form Fe^{II}—OH (Eq. (14)). After that, H_2O_2 undergoes catalytic decomposition to form Fe^{III}—OH and $^{\bullet}OH$ (Eq. (15)), which oxidize the organic pollutants, leading to the formation of intermediaries or complete mineralization to CO_2, water and inorganic ions (Eq. (16)).

$$\equiv Fe^{III}\text{–}OH + e^- \rightarrow Fe^{II}\text{–}OH \quad (11)$$

$$\equiv Fe^{III}\text{–}OH + H_2O_2 \leftrightarrow \equiv Fe^{III}\text{–}OH\left(H_2O_2\right)_{(s)} \quad (12)$$

$$\equiv Fe^{III}\text{–}OH\left(H_2O_2\right)_{(s)} \rightarrow \equiv Fe^{II}\text{–}OH\ \left(HO_2^{\bullet}\right)_{(s)} + H^+ \quad (13)$$

$$\equiv Fe^{II}\text{–}OH\ \left(HO_2\bullet\right)(s) \rightarrow \equiv Fe^{II}\text{–}OH + HO_2^{\bullet} + H^+ \quad (14)$$

$$\equiv Fe^{II}\text{–}OH + H_2O_2 \rightarrow \equiv Fe^{III}\text{–}OH + \bullet OH + OH^- \quad (15)$$

$$\bullet OH + \text{pollutant} \rightarrow \text{intermediaries} \rightarrow CO_2 + H_2O \quad (16)$$

Quenching experiments were performed using isopropanol ($^{\bullet}OH$ scavenger) in order to study the role of active species in the heterogeneous EF process under neutral pH (Fig. 7). The results obtained in these experiments showed that in the presence of isopropanol, NOR removal decreased from 100 to 58% in 30 min of reaction when the MCF/Fe-incorporated cathode was applied, while the MCF/Fe-deposited cathode recorded a decrease in NOR removal from 34.64 to 17.2%. The system equipped with the MCF cathode also recorded a decline in NOR removal from 23 to 11.1% (Santos et al. 2021). In the case of the MCF cathode, the reduction observed in the degradation rate can be attributed to the blockage of $^{\bullet}OH$ species on the DSA® anode surface — which produces the higher state

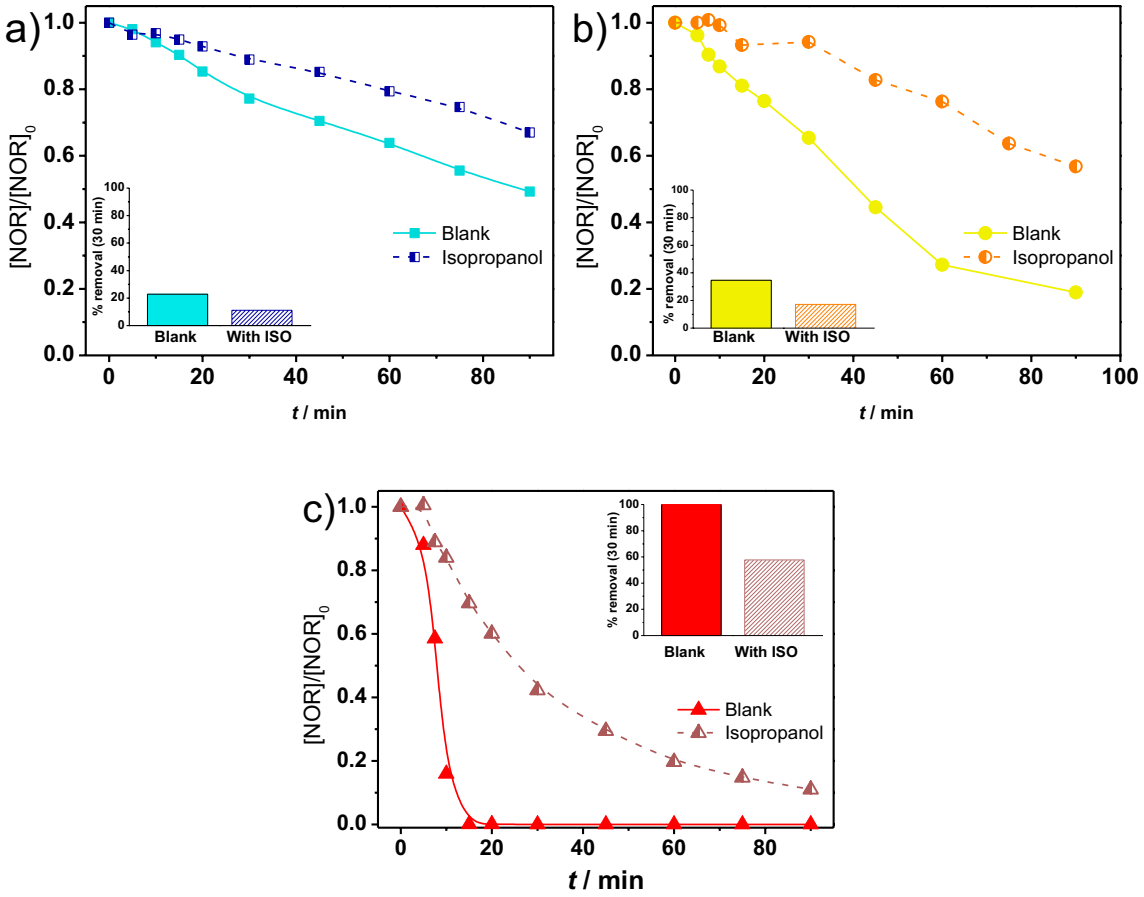

Fig. 7 Effect of •OH scavenger on the degradation of NOR during electrolysis using MCF (anodic oxidation) (**a**), MCF/Fe-deposited (**b**) and MCF/Fe-incorporated (**c**) electrodes

superoxide that is responsible for the partial oxidation of organic compounds (Martínez-Huitle and Andrade 2011; Martínez-Huitle et al. 2015).

It can be clearly observed that •OH species played a major role in the system equipped with the MCF/Fe-incorporated cathode; this points to the occurrence of a quick reaction between the deposited iron oxide (Fe^{III}/Fe^{II}) and the H_2O_2 electrogenerated *in situ* to produce highly reactive radicals on the cathode surface. On the other hand, the iron-deposited electrode exhibited a less pronounced reduction in degradation rate; this outcome can be related to the lower surface area of this electrode, as can be seen in the electrochemical characterization images/data. That is, iron oxide partially blocks the felt fibers (as can be seen in the SEM images in Fig. 3a), and this leads to a decrease in the ECSA value. Finally, in the case of the MCF-(3) electrode, the inhibition of NOR removal was found to be less pronounced; this means that anodic oxidation via direct electron transfer and HO• species on the anode surface is the main mechanism responsible for NOR degradation.

Overall, the possible mechanism involving NOR degradation via the application of the two different iron oxide–based cathodes prepared in this study appears to be the same; the surface reactions are found to be the main mechanism involved in NOR degradation under the HEF treatment process. The iron deposited or incorporated into the cathode yields $\equiv Fe^{II}$; this product in turn reacts to form H_2O_2 and O_2 which generate •OH and $O_2^{\bullet-}$. The •OH and $O_2^{\bullet-}$ generated then act to promote NOR degradation on the cathode surface, thus enhancing the degradation efficiency.

Reusability and leaching of the MCF/Fe-incorporated cathode

Reusability of the cathode is crucial to evaluate the cost-effectiveness and feasibility of the proposed process. In this view, cycling tests were performed using the MCF/Fe-incorporated cathode (Fig. SM4) and as can be observed, degradation efficiency does not decrease after four successive cycles (keeping 100% removal within 90 min

treatment). Although in neutral medium, Fe^{III} is expected to be insoluble; the contribution of dissolved iron must also be accounted in HEF systems even at neutral pH. Thus, a further investigation of iron leaches from the electrode surface was conducted (Fig. SM.5). As a result, the total iron measured at the end of the experiment was 2.36 ± 0.3 mg L^{-1} which shows a controlled leaching of iron in each cycle in the HEF system with MCF/Fe-incorporated electrode. For comparison, the value found for the MCF/Fe-deposited (0.17± 0.005 mg L^{-1}) is much lower. Clearly, the higher concentration of leached iron promotes the enhanced efficiency of HEF with MCF/Fe-incorporated for NOR degradation, as it would lead to a faster activation of H_2O_2 to produce radicals compared to MCF/Fe-deposited.

Conclusions

The present study reported the development of a novel synthesis technique, which involved the modification of CF with PL6C/PTFE and iron oxide (deposited or incorporated) and the application of the modified CF electrode in HEF system for the treatment of water contaminated by recalcitrant and hazardous compounds, including antibiotics. The main conclusions drawn from this study are as follows:

- Increasing PL6C/PTFE loading does not cause a significant effect on H_2O_2 electrogeneration. The modification of CF with only 3 mg cm^{-3} catalyst loading led to the generation of sufficient active sites for H_2O_2 electrogeneration with higher current efficiency.
- Both iron-based cathodes investigated in this study were synthesized successfully; the iron oxides were homogenously dispersed on the carbon felt fibers. The one-step synthesis approach (i.e., MCF/Fe-incorporated) was found to be the best route for the construction of highly efficient iron-modified CF in terms of morphology with homogenous deposition of iron oxide without losing the 3D character and electrochemical properties (highest ECSA and greater conductivity).
- After the modification of CF with iron, a decrease was observed in H_2O_2 production due to the quick reaction of H_2O_2 with the iron to form $^{\bullet}OH$ species. For the degradation experiments performed under neutral pH, the MCF/Fe-incorporated cathode exhibited the best efficiency in terms of NOR removal, mineralization and energy consumption.
- From mechanistic study, the coexistence of heterogeneous (surface reactions) and homogeneous reactions (activation of H_2O_2 in solution by the iron leached) helps to explain the outstanding degradation results exhibited by the MCF/Fe-incorporated cathode.
- Recyclability of MCF-Fe incorporated with controlled iron leaching points out that heterogeneous supported iron can be used in several consecutive cycles proving that cathode easy-to-prepare is a suitable alternative material for the degradation of contaminants from aqueous solutions.

Finally, the application of the iron-modified carbon-based materials, prepared by a simple, facile and low-cost methodology, under the HEF treatment process is a highly efficient alternative technique for the degradation and mineralization of organic pollutants in aqueous medium under pH conditions close to neutral; this technique helps expand the application range of the treatment process.

Supplementary Information The online version contains supplementary material available at https://doi.org/10.1007/s11356-023-30536-2.

Author contribution All authors contributed to the conception and design of the study. All authors contributed to the conception and design of the study. Material preparation, data collection, and analysis were performed by Gessica O. S Santos, Lorena A. Goulart, Isaac Sánchez-Montes. The first draft of the manuscript was written by Gessica O. S. Santos. Writing—review and editing by Lorena A. Goulart, Isaac Sánchez-Montes, Ronaldo S. Silva and Marcos R. V. Lanza and commented on previous versions of the manuscript. Resources by Ronaldo S. Silva and Marcos R. V Lanza. Acquisition of the financial support and supervision by Marcos R. V. Lanza. All authors read and approved the final manuscript.

Funding The authors are grateful to the São Paulo Research Foundation (FAPESP – grants #2017/10118-0, #2014/50945-4, #2016/08760, #2020/02743-4 and #2020/07351-7), National Council for Scientific and Technological Development - CNPq (grant#303943/2021-1) and CAPES-Finance Code 001 for the financial assistance provided in support of this work.

Data availability Data will be made available on request.

Declarations

Consent to participate Not applicable (this study does not contain any individual person's data in any form).

Consent for publication The authors declare that they agree with the publication of this paper in this journal.

Conflict of interest The authors declare no competing interests.

References

Abaalkhail AA, Alshammari BA, Almutairi GN, Alenazey FS, Alotibi MF, Alenad AM, Alharbi AG, Almoneef TS, AlOtaibi BM (2022) Enhancing the performance of a metal-free self-supported carbon felt-based supercapacitor with facile two-step electrochemical activation. Nanomaterials 12:427

Alizadeh Z, Rezaee A (2022) Tetracycline removal using microbial cellulose@ nano-Fe3O4 by adsorption and heterogeneous Fenton-like processes. J Mol Liquids 366:120199

Annabi C, Fourcade F, Soutrel I, Geneste F, Floner D, Bellakhal N, Amrane A (2016) Degradation of enoxacin antibiotic by the electro-Fenton process: optimization, biodegradability improvement and degradation mechanism. J Environ Manag 165:96–105

Barhoumi N, Labiadh L, Oturan MA, Oturan N, Gadri A, Ammar S, Brillas E (2015) Electrochemical mineralization of the antibiotic levofloxacin by electro-Fenton-pyrite process. Chemosphere 141:250–257

Barros WR, Ereno T, Tavares AC, Lanza MR (2015a) In situ electrochemical generation of hydrogen peroxide in alkaline aqueous solution by using an unmodified gas diffusion electrode. ChemElectroChem 2:714–719

Barros WRP, Ereno T, Tavares AC, Lanza MRV (2015b) In situ electrochemical generation of hydrogen peroxide in alkaline aqueous solution by using an unmodified gas diffusion electrode. ChemElectroChem 2:714–719

Bolton JR, Bircher KG, Tumas W, Tolman CA (1996) Figures-of-merit for the technical development and application of advanced oxidation processes. J Adv Oxid Technol 1:13–17

Bolton JR, Bircher KG, Tumas W, Tolman CA (2001) Figures-of-merit for the technical development and application of advanced oxidation technologies for both electric-and solar-driven systems (IUPAC Technical Report). Pure Appl Chem 73:627–637

Brillas E, Bastida RM, Llosa E, Casado J (1995) Electrochemical destruction of aniline and 4-chloroaniline for wastewater treatment using a carbon-PTFE O 2-fed cathode. J Electrochem Soc 142:1733

Brillas E, Sirés I, Oturan MA (2009) Electro-Fenton process and related electrochemical technologies based on Fenton's reaction chemistry. Chem Rev 109:6570–6631

Carneiro JF, Aquino JM, Silva BF, Silva AJ, Rocha-Filho RC (2020) Comparing the electrochemical degradation of the fluoroquinolone antibiotics norfloxacin and ciprofloxacin using distinct electrolytes and a BDD anode: evolution of main oxidation byproducts and toxicity. J Environ Chem Eng 8:104433

Carneiro JF, Paulo MJ, Siaj M, Tavares AC, Lanza MR (2015) Nb2O5 nanoparticles supported on reduced graphene oxide sheets as electrocatalyst for the H2O2 electrogeneration. J Catal 332:51–61

Cordeiro-Junior PJM, Kronka MS, Goulart LA, Verissimo NC, Mascaro LH, dos Santos MC, Bertazzoli R, de Vasconcelos Lanza MR (2020) Catalysis of oxygen reduction reaction for H2O2 electrogeneration: the impact of different conductive carbon matrices and their physicochemical properties. J Catal 392:56–68

Forti J, Rocha R, Lanza M, Bertazzoli R (2007) Electrochemical synthesis of hydrogen peroxide on oxygen-fed graphite/PTFE electrodes modified by 2-ethylanthraquinone. J Electroanal Chem 601:63–67

Fortunato GV, Kronka MS, dos Santos AJ, Ledendecker M, Lanza MR (2020a) Low Pd loadings onto Printex L6: synthesis, characterization and performance towards H2O2 generation for electrochemical water treatment technologies. Chemosphere 259:127523

Fortunato GV, Kronka MS, dos Santos AJ, Ledendecker M, Lanza MRV (2020b) Low Pd loadings onto Printex L6: synthesis, characterization and performance towards H2O2 generation for electrochemical water treatment technologies. Chemosphere 259:127523

Ganiyu SO, Martínez-Huitle CA, Oturan MA (2021) Electrochemical advanced oxidation processes for wastewater treatment: advances in formation and detection of reactive species and mechanisms. Curr Opin Electrochem 27:100678

Ganiyu SO, Zhou M, Martinez-Huitle CA (2018) Heterogeneous electro-Fenton and photoelectro-Fenton processes: a critical review of fundamental principles and application for water/wastewater treatment. Appl Catal B: Environ 235:103–129

Ghanbari F, Hassani A, Wacławek S, Wang Z, Matyszczak G, Lin K-YA, Dolatabadi M (2021) Insights into paracetamol degradation in aqueous solutions by ultrasound-assisted heterogeneous electro-Fenton process: key operating parameters, mineralization and toxicity assessment. Sep Purif Technol 266:118533

Han Z, Li Z, Li Y, Shang D, Xie L, Lv Y, Zhan S, Hu W (2022) Enhanced electron transfer and hydrogen peroxide activation capacity with N, P-codoped carbon encapsulated CeO2 in heterogeneous electro-Fenton process. Chemosphere 287:132154

Huang A, Zhi D, Zhou Y (2021) A novel modified Fe–Mn binary oxide graphite felt (FMBO-GF) cathode in a neutral electro-Fenton system for ciprofloxacin degradation. Environ Pollut 286:117310

Jonoush ZA, Rezaee A, Ghaffarinejad A (2020) Electrocatalytic nitrate reduction using Fe0/Fe3O4 nanoparticles immobilized on nickel foam: selectivity and energy consumption studies. J Clean Prod 242:118569

Jonoush ZA, Rezaee A, Ghaffarinejad A (2021) Enhanced electrocatalytic denitrification using non-noble Ni-Fe electrode supplied by Fe3O4 nanoparticle and humic acid. Appl Surf Sci 563:150142

Jonoush ZA, Rezaee A, Ghaffarinejad A (2022) Electrocatalytic disinfection of E. coli using Ni-Fe/Fe3O4 nanocomposite cathode: effect of Fe3O4 nanoparticle, humic acid, and nitrate. Sep Purif Technol 294:121140

Kabtamu DM, Lin G-Y, Chang Y-C, Chen H-Y, Huang H-C, Hsu N-Y, Chou Y-S, Wei H-J, Wang C-H (2018) The effect of adding Bi 3+ on the performance of a newly developed iron–copper redox flow battery. RSC Adv 8:8537–8543

Karatas O, Gengec NA, Gengec E, Khataee A, Kobya M (2022) High-performance carbon black electrode for oxygen reduction reaction and oxidation of atrazine by electro-Fenton process. Chemosphere 287:132370

Kasonga TK, Coetzee MA, Kamika I, Ngole-Jeme VM, Momba MNB (2021) Endocrine-disruptive chemicals as contaminants of emerging concern in wastewater and surface water: a review. J Environ Manag 277:111485

Khan AH, Khan NA, Ahmed S, Dhingra A, Singh CP, Khan SU, Mohammadi AA, Changani F, Yousefi M, Alam S (2020) Application of advanced oxidation processes followed by different treatment technologies for hospital wastewater treatment. J Clean Prod 269:122411

Kim KJ, Lee S-W, Yim T, Kim J-G, Choi JW, Kim JH, Park M-S, Kim Y-J (2014) A new strategy for integrating abundant oxygen functional groups into carbon felt electrode for vanadium redox flow batteries. Sci Rep 4:1–6

Kovalakova P, Cizmas L, McDonald TJ, Marsalek B, Feng M, Sharma VK (2020) Occurrence and toxicity of antibiotics in the aquatic environment: a review. Chemosphere 251:126351

Lanzarini-Lopes M, Garcia-Segura S, Hristovski K, Westerhoff P (2017) Electrical energy per order and current efficiency for electrochemical oxidation of p-chlorobenzoic acid with boron-doped diamond anode. Chemosphere 188:304–311

Le TXH, Bechelany M, Cretin M (2017) Carbon felt based-electrodes for energy and environmental applications: A review. Carbon 122:564–591

Li X, Xiao C, Ruan X, Hu Y, Zhang C, Cheng J, Chen Y (2022) Enrofloxacin degradation in a heterogeneous electro-Fenton system using a tri-metal-carbon nanofibers composite cathode. Chem Eng J 427:130927

Li Z-L, Cheng R, Chen F, Lin X-Q, Yao X-J, Liang B, Huang C, Sun K, Wang A-J (2021) Selective stress of antibiotics on microbial denitrification: inhibitory effects, dynamics of microbial community structure and function. J Hazard Mater 405:124366

Liang C, Su H-W (2009) Identification of sulfate and hydroxyl radicals in thermally activated persulfate. Ind Eng Chem Res 48:5558–5562

Liu Y, Gao C, Liu L, Yu T, Li Y (2022) Improved degradation of tetracycline, norfloxacin and methyl orange wastewater treatment with dual catalytic electrode assisted self-sustained Fe2+ electro-Fenton system: regulatory factors, mechanisms and pathways. Sep Purif Technol 284:120232

Luo H, Zeng Y, He D, Pan X (2021) Application of iron-based materials in heterogeneous advanced oxidation processes for wastewater treatment: a review. Chem Eng J 407:127191

Martínez-Huitle CA, Andrade LS (2011) Electrocatalysis in wastewater treatment: recent mechanism advances. Quimica Nova 34:850–858

Martínez-Huitle CA, Rodrigo MA, Sirés I, Scialdone O (2015) Single and coupled electrochemical processes and reactors for the abatement of organic water pollutants: a critical review. Chem Rev 115:13362–13407

McCrory CC, Jung S, Peters JC, Jaramillo TF (2013) Benchmarking heterogeneous electrocatalysts for the oxygen evolution reaction. J Am Chem Soc 135:16977–16987

Médice RV, Afonso RJCF, Almeida MLB, de Aquino SF, Libânio M (2021) Preliminary assessment of antimicrobial activity and acute toxicity of norfloxacin chlorination by-product mixture. Environ Sci Pollut Res 28:3828–3836

Michael I, Rizzo L, McArdell C, Manaia C, Merlin C, Schwartz T, Dagot C, Fatta-Kassinos D (2013) Urban wastewater treatment plants as hotspots for the release of antibiotics in the environment: a review. Water Res 47:957–995

Mohamed HO, Obaid M, Poo K-M, Abdelkareem MA, Talas SA, Fadali OA, Kim HY, Chae K-J (2018) Fe/Fe2O3 nanoparticles as anode catalyst for exclusive power generation and degradation of organic compounds using microbial fuel cell. Chem Eng J 349:800–807

Mora-Gómez J, Ortega E, Mestre S, Pérez-Herranz V, García-Gabaldón M (2019) Electrochemical degradation of norfloxacin using BDD and new Sb-doped SnO2 ceramic anodes in an electrochemical reactor in the presence and absence of a cation-exchange membrane. Sep Purif Technol 208:68–75

Munoz M, De Pedro ZM, Casas JA, Rodriguez JJ (2015) Preparation of magnetite-based catalysts and their application in heterogeneous Fenton oxidation–a review. Appl Catal B: Environ 176:249–265

Murti GK, Moharir A, Sarma V (1970) Spectrophotometric determination of iron with orthophenanthroline. Microchem J 15:585–589

Paz EC, Aveiro LR, Pinheiro VS, Souza FM, Lima VB, Silva FL, Hammer P, Lanza MR, Santos MC (2018) Evaluation of H2O2 electrogeneration and decolorization of Orange II azo dye using tungsten oxide nanoparticle-modified carbon. Appl Catal B: Environ 232:436–445

Perry SC, Pangotra D, Vieira L, Csepei L-I, Sieber V, Wang L, Ponce de León C, Walsh FC (2019) Electrochemical synthesis of hydrogen peroxide from water and oxygen. Nat Rev Chem 3:442–458

Petrucci E, Da Pozzo A, Di Palma L (2016) On the ability to electrogenerate hydrogen peroxide and to regenerate ferrous ions of three selected carbon-based cathodes for electro-Fenton processes. Chem Eng J 283:750–758

Pironti C, Ricciardi M, Proto A, Bianco PM, Montano L, Motta O (2021) Endocrine-disrupting compounds: an overview on their occurrence in the aquatic environment and human exposure. Water 13:1347

Ren H, Pan Y, Sorrell CC, Du H (2020) Assessment of electrocatalytic activity through the lens of three surface area normalization techniques. J Mater Chem A 8:3154–3159

Rofaiel A, Ellis J, Challa P, Bazylak A (2012) Heterogeneous through-plane distributions of polytetrafluoroethylene in polymer electrolyte membrane fuel cell gas diffusion layers. J Power Sources 201:219–225

Samanta C (2008) Direct synthesis of hydrogen peroxide from hydrogen and oxygen: an overview of recent developments in the process. Appl Catal A: General 350:133–149

Santos GO, Vasconcelos VM, da Silva RS, Rodrigo MA, Eguiluz KI, Salazar-Banda GR (2020) New laser-based method for the synthesis of stable and active Ti/SnO2–Sb anodes. Electrochim Acta 332:135478

Santos GOS, Dória AR, da Silva Almeida CV, Pupo M, Da Silva RS, Eguiluz KIB, Salazar-Banda GR (2021) Understanding the effect of the high hydrophobicity of the laser-prepared Ti/SnO 2–Sb–La 2 O 3 anode on its electrocatalytic properties. Mater Adv 2:4016–4028

Shi T, Peng J, Chen J, Sun C, He H (2017) Heterogeneous photo-fenton degradation of norfloxacin with Fe3O4-multiwalled carbon nanotubes in aqueous solution. Catal Lett 147:1598–1607

Sirés I, Brillas E (2021) Upgrading and expanding the electro-Fenton and related processes. Curr Opin Electrochem 27:100686

Soltani R, Rezaee A, Khataee A, Godini H (2013) Electrochemical generation of hydrogen peroxide using carbon black-, carbon nanotube-, and carbon black/carbon nanotube-coated gas-diffusion cathodes: effect of operational parameters and decolorization study. Res Chem Intermediates 39:4277–4286

Su P, Zhou M, Ren G, Lu X, Du X, Song G (2019) A carbon nanotube-confined iron modified cathode with prominent stability and activity for heterogeneous electro-Fenton reactions. J Mater Chem A 7:24408–24419

Taoufik N, Boumya W, Achak M, Sillanpää M, Barka N (2021) Comparative overview of advanced oxidation processes and biological approaches for the removal pharmaceuticals. J Environ Manag 288:112404

Van Doorslaer X, Dewulf J, Van Langenhove H, Demeestere K (2014) Fluoroquinolone antibiotics: an emerging class of environmental micropollutants. Sci Total Environ 500:250–269

Wan Z, Wang J (2017) Degradation of sulfamethazine using Fe3O4-Mn3O4/reduced graphene oxide hybrid as Fenton-like catalyst. J Hazard Mater 324:653–664

Wang G, Wang H, Lu X, Ling Y, Yu M, Zhai T, Tong Y, Li Y (2014) Solid-state supercapacitor based on activated carbon cloths exhibits excellent rate capability. Adv Mater 26:2676–2682

Wang G, Zhao D, Kou F, Ouyang Q, Chen J, Fang Z (2018) Removal of norfloxacin by surface Fenton system (MnFe2O4/H2O2): kinetics, mechanism and degradation pathway. Chem Eng J 351:747–755

Wang Y, Zhao G, Chai S, Zhao H, Wang Y (2013) Three-dimensional homogeneous ferrite-carbon aerogel: one pot fabrication and enhanced electro-Fenton reactivity. ACS Appl Mater Interfaces 5:842–852

Wang Z, Liu M, Xiao F, Postole G, Zhao H, Zhao G (2021) Recent advances and trends of heterogeneous electro-Fenton process for wastewater treatment-review. Chinese Chem Lett 33:653–662

Ye D, Yu Y, Tang J, Liu L, Wu Y (2016) Electrochemical activation of carbon cloth in aqueous inorganic salt solution for superior capacitive performance. Nanoscale 8:10406–10414

Yi L, Li B, Sun Y, Li S, Qi Q, Qin J, Sun H, Wang X, Wang J, Fang D (2021) Degradation of norfloxacin in aqueous solution using hydrodynamic cavitation: optimization of geometric and operation parameters and investigations on mechanism. Sep Purif Technol 259:118166

Yu F, Zhou M, Yu X (2015) Cost-effective electro-Fenton using modified graphite felt that dramatically enhanced on H2O2 electro-generation without external aeration. Electrochim Acta 163:182–189

Zhang Q, Zhou M, Ren G, Li Y, Li Y, Du X (2020) Highly efficient electrosynthesis of hydrogen peroxide on a superhydrophobic three-phase interface by natural air diffusion. Nat Commun 11:1–11

Zhou M, Yu Q, Lei L (2008) The preparation and characterization of a graphite–PTFE cathode system for the decolorization of CI Acid Red 2. Dyes Pigments 77:129–136

Zhou W, Meng X, Gao J, Alshawabkeh AN (2019) Hydrogen peroxide generation from O2 electroreduction for environmental remediation: a state-of-the-art review. Chemosphere 225:588–607